National Aeronautics and Space Administration

Xilinx V4 Package Reliability: Properties and Reliability of LP2 Underfill Material

Jong-ook Suh
Jet Propulsion Laboratory
Pasadena

R. Peter Dillon
Jet Propulsion Laboratory
Pasadena

Jet Propulsion Laboratory
California Institute of Technology
Pasadena, California

JPL Publication 12-6 3/12

National Aeronautics and Space Administration

Xilinx V4 Package Reliability: Properties and Reliability of LP2 Underfill Material

NASA Electronic Parts and Packaging (NEPP) Program
Office of Safety and Mission Assurance

Jong-ook Suh
Jet Propulsion Laboratory
Pasadena

R. Peter Dillon
Jet Propulsion Laboratory
Pasadena

NASA WBS: 724297.40.49.11
JPL Project Number: 104593
Task Number: 40.49.02.13

Jet Propulsion Laboratory
4800 Oak Grove Drive
Pasadena, CA 91109

http://nepp.nasa.gov

This research was carried out at the Jet Propulsion Laboratory, California Institute of Technology, and was sponsored by the National Aeronautics and Space Administration Electronic Parts and Packaging (NEPP) Program.

TABLE OF CONTENTS

1.0 INTRODUCTION

The Xilinx Virtex 4 (V4) is a next-generation field programmable gate array (FPGA) candidate for use on future NASA flight projects. The Virtex 4 is a state-of-the-art radiation-tolerant SRAM-based (reconfigurable) FPGA. It is manufactured using a 90-nm CMOS process at the United Microelectronics Corporation (UMC) wafer foundry in Taiwan. A cartoon of the V4 ceramic flip chip package is shown in the Figure 1-1. High lead (90Pb/10Sn) solder columns are attached to the substrate while higher lead (95Pb/5Sn) solder bumps are arranged across the surface of the flip chip die. The bumped die is flipped and reflowed to an alumina ceramic substrate. A moisture resistant epoxy underfill encapsulates the solder bumps; however the Xilinx V4 is non-hermetically packaged and, thus, directly exposes the underfill to the external environment.

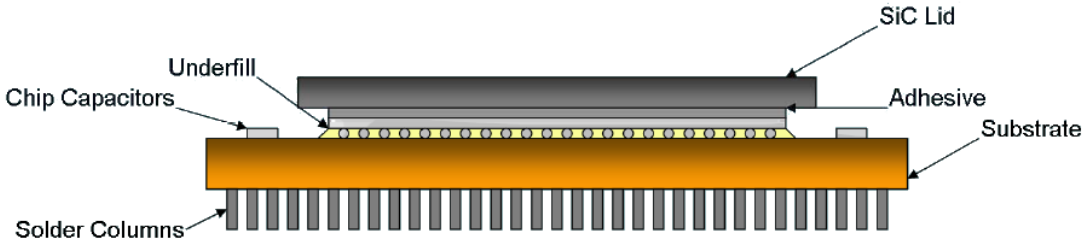

Figure 1-1. Schematic structure of Xilinx V4

At this time, the Virtex-4 is not qualified to MIL-PRF-38535 Qualified Manufacturer Listing (QML) Level V. QML space-level certification of the V4 by Defense Supply Center Columbus (DSCC) to MIL-PRF-38535 QML Level V is still in progress. It should be noted that MIL-PRF-38535 has only been defined for hermetic ceramic packages. Since V4s are non-hermetic Ceramic Column Grid Array (CGA) flip chips, there has been continuing debate between the space community and DSCC whether to introduce a new class for non-hermetic space-level products [1]. Before NASA certifies the V4 for use in space flight applications, reliability concerns related to the non-hermeticity of the V4 need to be addressed.

A significant amount of testing of the V4 construction has been performed to date. These tests have been primarily mil-spec reliability tests, such as thermal cycling, moisture preconditioning, and outgassing. In spite of the non-hermetic packaging, the V4 performed well during those tests; however, the testing performed to date has not been interpreted for NASA applications (e.g., NASA-relevant environments). Additionally, review of the underfill, a significant contributor to the reliability of the V4, and its performance in NASA-relevant environments has been limited. The objective of the present study is to investigate the reliability of the underfill as it relates to protecting the flip chip/solder bump/substrate interface when exposed to NASA relevant environments (e.g., low-Earth orbit [LEO]). The existing reliability test results are evaluated and interpreted for environments important to NASA as they relate to the reliability of the interface described above.

1.1 Roll of Underfill on Reliability of Flip Chip Packages

1.1.1 Stress in Flip Chip Solder Joints

One of the major reliability-limiting factors of flip chip solder joints is solder fatigue by thermal/power cycling. The fatigue stress mainly originates from Coefficient of Thermal Expansion (CTE) mismatch between the die and the substrate material. The solder joints are subjected to stress by thermal expansion during the reflow. This is schematically depicted in the Figure 1-2 [2].

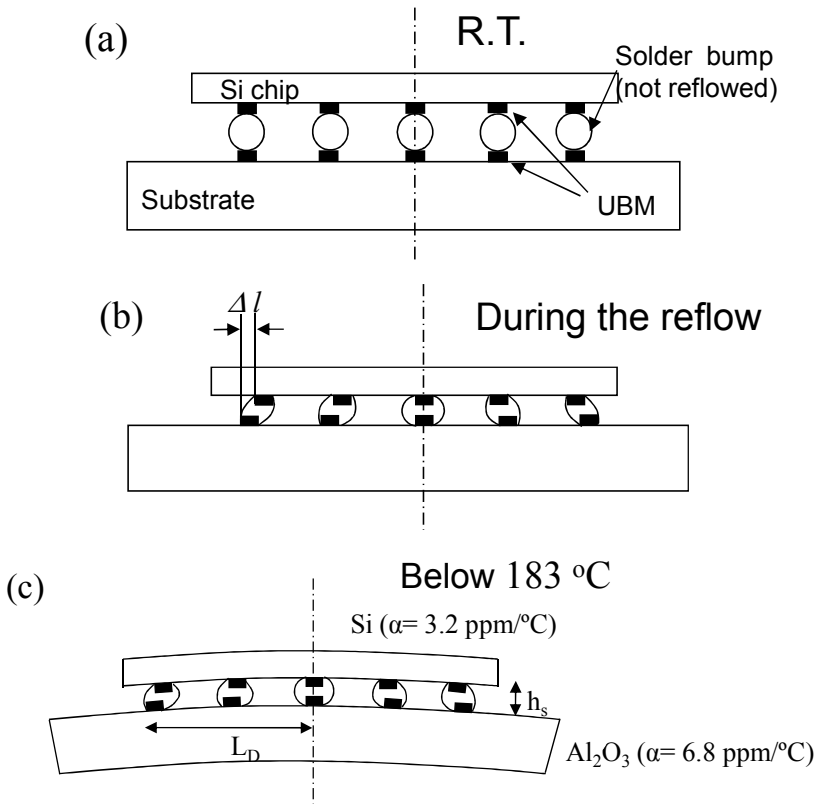

Figure 1-2. Schematic diagram of a flip chip under stress (a) at room temperature before reflow, (b) during the reflow, and (c) at temperature below the melting temperature of the eutectic SnPb solder.

Substrate materials usually have a CTE greater than that of the die. Before solder reflow there is no thermal stress. During reflow, which takes place at a temperature >200ºC, the substrate expands more than the die. There is no thermal stress on solder, however, because the solder is in a molten state. Following completion of solder reflow the entire assembly is cooled and the solder solidifies and becomes rigid once the temperature falls below the solder's solidus temperature. The solidified solder bumps act to prevent the upper surface of the substrate from shrinking. The substrate bends concavely downward, resulting in a shear stress on the solder joints. The solder joint at the corner of the die experiences the largest possible shear strain (γ_{max}), which is given as [3]:

$$\gamma_{\max} = \frac{L_D}{h_s} \Delta\alpha \Delta T \tag{1}$$

where h_s is height of the solder joint, $\Delta\alpha$ is CTE difference, ΔT is the temperature difference between cold cycle and hot cycles, and L_D is half of the diagonal length of the die. Since the current industry trends are to reduce solder bump size, to use larger die and to use inexpensive organic substrates (which have larger CTEs), future solder joints will be subjected to larger stresses than previously observed. Use of low-k dielectric materials makes the situation worse as low-k materials are brittle. A low-k material can crack right after reflow, before applying underfill, due to its low toughness. In order to reduce stress in flip chip solder joints, one of the current industry approaches is to use tall copper pillars under solder bumps to increase h_s. Use of the copper pillar bumps increases the resistance to electromigration [4].

Without mitigation, increases in γ_{max} will result in shorter fatigue life. The mean cycles to failure, Nf, can be roughly expressed as:

$$N_f \approx K\gamma_{\max}^{1/c} \approx K(\frac{L_D}{h_s}\Delta\alpha\Delta T)^{-2.3} \quad (2)$$

which is a simplified expression of a modified Manson-Coffin equation by Engelmaier [5]. K is a constant composed of various factors such as an empirical constant, the fatigue ductility coefficient, and the Weibull shape parameter. The value, c, is the so-called fatigue ductility exponent, and $1/c$ is approximately –2.3.

As in equation (2), the fatigue life of the flip chip solder bumps furthest from the center of the die, the distance specified by L_D, decreases for larger die (i.e., increasing L_D). Smaller solder joints will tend to have shorter fatigue life, because of small value of h_s. If the CTE of the substrate material is increasingly different from the CTE of the die material, $\Delta\alpha$ will increase, again decreasing the fatigue life. In summary, use of larger die, smaller solder interconnects, and substrates with larger CTE mismatch to the die will limit the reliability of a flip chip assembly. An early mitigator of these limitations was to use a silicone conformal coating or evaporated Parylene at surfaces of the flip chip cavity, which increased thermal cycling reliability by 50–100% [6]. It is the use of underfill, however, which further increased the reliability and nearly eliminated the flip chip solder interconnect fatigue issue.

Flip chips with a size of 6.5 × 6.5 mm attached to Al_2O_3 chip carriers without underfill exhibited 50% interconnection failure (N_{50}) after about 1300 cycles during thermal cycling of –55 to +125ºC. There were not enough failures in 10,000 cycles to calculate N_{50} when an underfill was used [7]. Among all the materials used as substrate, Al_2O_3 has been proven to be the most reliable in regards to the solder joint fatigue life [6]. If an organic substrate is used instead of alumina solder joints can fail within 1000 cycles during thermal cycling of –55 to 125ºC, even in the presence of the underfill. This is due to the higher CTE of the organic substrate as compared to alumina.

Flip chip solder joints are subjected to shear-dominant loading. The joints farthest from the center of the die experience the greatest strains and fatigue the fastest. The underfill creates a monolithic structure by coupling the silicon die and the substrate, minimizing the stress on the solder joints. Underfills redistribute the stresses over the entire plane of underfill rather than allow stress concentration at the solder joints. Without the underfill, the stress on the flip chip solder interconnects could be said to be equal to the force divided by the total cross-sectional area of solder bumps. By applying the underfill, the stress becomes the force divided by the total area of the die. In other words, the shear stress on the joints becomes uniform over the entire die area resulting in significantly reduced stress on each solder joints. To be more precise, the underfill changes the dominant strain from shear to axial or longitudinal, inducing hydrostatic compressive stresses on the solder joints. Instead of the solder joints, the underfill essentially carries most of the stress. The reduction of stress on solder joints is more than an order of magnitude. The traditional solder joint fatigue model, such as the one in equation 2, is therefore not effective when predicting failure of underfilled flip chips. For underfilled flip chip assemblies, breakdown of the underfill determines the failure rate instead of solder. Failure of flip chip solder joints with an underfill generally occur after the underfill material becomes compromised.

There are several finite element modeling studies indicating that the dependence of solder fatigue life on the size of the die can be completely eliminated by using an underfill. This does not necessarily mean that die of any size can be used if underfill is applied. Stress evolution in solder joints resulting from the solder reflow process will factor into the maximum reliable die size.

1.1.2 Relationship Between Underfill and Hermeticity in Electronic Packaging

For commercial applications, an underfilled flip chip package does not need hermetic packaging [8] and most commercial flip chip packages today are non-hermetic. One of the reasons is because the underfill provides enough environmental protection for the interconnections. Before the introduction of underfill, single-chip or multi-chip modules were hermetically sealed. The hermetic sealing improved reliability

and lengthened the fatigue life of solder joints by minimizing interaction between the environment and the solder interconnects. Introduction of underfill, however, provided similar environmental protection with improved stress relief. This eliminated the need for hermetic sealing and enabled the reliable packaging of larger dies. The result has been reduced cost and size for modules; most non-hermetic packages today use an underfill.

1.1.3 Properties of Underfill as Related to Key Reliability Issues Relevant to NASA Missions

The major contribution of underfill to reliabile flip chip solder joints is stress redistribution. The most important material properties that affect an underfill's capacity for stress redistribution are adhesion, elastic modulus (E), CTE, and glass transition temperature (Tg) [6].

Underfill adhesion is considered to be the most important factor affecting the reliability of flip chip assemblies [6]. As stated above, the underfill carries most of the CTE mismatch stress instead of the solder joints. This can only be realized if the underfill maintains good adhesion to the other materials. In a flip chip package, the underfill material needs to have good adhesion with many different material surfaces, including the solder, die passivation, the substrate, and the die edges. The previously stated industry trend of larger, denser (i.e., increased I/O count) flip chips increases the stress on the solder joints and leads to a shorter fatigue life. The introduction of underfill improved the fatigue life of flip chip solder interconnects by 5 to 10 times or more. If the underfill does not have proper adhesion strength, however, underfill cracking, underfill delamination, or chip cracking can be caused by the stress. An underfill cannot effectively reduce solder fatigue if there are cracks or delamination. Since the materials used in a flip chip package varies from case to case, the underfill chemistry needs be engineered accordingly. Good adhesion also needs to be maintained even in the presence of contaminants, such as flux residue. Finally, an underfill also needs to be able to maintain adhesion after exposure to adverse environmental conditions such as thermal cycling and/or moisture exposure.

The elastic modulus (E) of the underfill should be sufficiently large to prevent stress concentrations in the solder bumps without exerting excessive stress on the die. According to a finite element model, the elastic modulus of an underfill should be as high as possible for the known adhesion strength [9]. Underfills with an elastic modulus greater than 1 Mpsi (6.89 GPa) can easily transmit load to the substrate and reduce strains of the solder joints [6]. The elastic modulus varies according to temperature. The elastic modulus of an underfill also undergoes a large change at the glass transition temperature, Tg. Above Tg, the elastic modulus tends to drop several orders of magnitude.

In terms of a contribution to the stress redistribution, the CTE is considered to be less important than adhesion or elastic modulus. For space applications, however, the importance of the underfill's CTE is increased as space applications often involve thermal cycling with large ΔTs. In order to minimize the amount of stress from thermal cycling, an ideal underfill material should have a CTE close to or slightly higher than the CTE of the solder [9]. The CTEs of typical epoxy resins, the base material of flip chip underfills, are typically between 50–70 ppm/ºC. The CTEs of solder alloys, however, are from 20–30 ppm/ºC (eutectic SnPb: 28.1 ppm/ºC, Sn3.5Cu0.7Ag: 20.4 ppm/ºC [10], 95Pb5Sn 29.0 ppm/ºC [11]). The CTE of an underfill can be controlled by adding the proper amount of a filler material, typically SiO_2. Addition of 60–70 wt% filler can reduce the CTE to 25–30 ppm/ºC [6]. An excess amount of filler will reduce the adhesion of the underfill since it will decrease the amount of epoxy resin at the bond surface. Like the modulus, the CTE of an underfill varies according to temperature. The change of the CTE is rather small at temperatures below the glass transition temperature, Tg. Above Tg the CTE increases rather rapidly.

As discussed above, large changes in elastic modulus and CTE occur at the Tg. Other properties, such as heat capacity and chemical resistance, tend to decrease at temperatures above Tg. Therefore Tg should be somewhat higher than the upper service temperature of the package.

2.0 LOW EARTH ORBIT (LEO) ENVIRONMENT AND RELEVANCE TO UNDERFILL PERFORMANCE

In the low Earth orbit (LEO) space environment, materials face harsh conditions such as extreme thermal cycling, high vacuum, atomic oxygen, UV radiation, and ionizing radiation (electrons, protons). Exposure of polymers such as an epoxy underfill to the LEO environment can result in degradation of the material and its properties. Surface erosion and modification of material properties (chemical, mechanical, electrical, thermal) can take place. As discussed previously, the properties and chemistry of an underfill are tailored for good adhesion and the proper mechanical properties. Modification of these properties by the environment may lead to undesirable effects such as loss of adhesion or change in elastic modulus and CTE.

2.1 LEO Environment

The major constituents of the LEO environment are high vacuum, ionizing radiation, atomic oxygen (ATOX), and UV radiation. There are also micrometeroids and orbital debris (MMOD), but the effect of MMOD will not be considered in the current study since electronic parts are expected to be well shielded from them. The other environmental effects are discussed below [12].

2.2 High Vacuum

The vacuum inside satellites at LEO is typically 10^{-6} to 10^{-7} Torr. The vacuum can induce outgassing of volatile components from polymers. The volatile components are mainly low-molecular weight fragments, additives, and absorbed gases. Besides contamination of sensitive optics and sensor surfaces, the outgassing can also result in the degradation of polymeric materials, especially at an elevated temperature.

2.3 Ionizing Radiation

The principal kinds of high-energy radiation are galactic cosmic rays, the geomagnetically trapped radiation at radiation belts (Van Allen radiation), and particles from solar flares (solar origin cosmic rays). Overall, the major constituents of ionizing radiation are high-energy electrons (up to several MeV), protons (up to several hundreds of MeV), alpha particles, heavy ions and high-energy photons. The galactic cosmic radiation consists mainly of very energetic penetrating protons and ions. Their intensity, however, is very small (less than 20 rads/year). The Van Allen radiation is more intense. It consists mainly of fast electrons (several tens of keV) and protons (tens or hundreds of MeV). The fast electrons can easily be eliminated by shielding. The proton dosage inside the shielding, though, is still about 100 rads/hr, which is high enough to damage semiconductor devices. The intensity and energy of the proton and alpha particle emission associated with solar flares can be very great, even under shielding (25 rads/hr, several hundreds of MeV). These energetic particles can degrade polymeric materials, electronic components, and solar cells by atomic displacement, ionization, and photon excitations.

2.4 Atomic Oxygen (ATOX)

ATOX is formed by photo-dissociation of O_2. ATOX constitutes 80% of the neutral atmosphere at LEO, and it is a severe hazard for polymeric materials. The density of ATOX is from 2×10^9 to 8×10^9 atoms/cm^3, depending on solar activity. The surface of a spacecraft facing the impingement direction experiences ATOX with kinetic energy of approximately 5 eV. The amount of the ATOX flux is about 10^{14} to 10^{15} atoms/cm^2 sec. According to existing studies, ATOX can react with polymers and cause chemical composition change, surface erosion, surface morphology change, and changes in optical properties. It is generally expected that electronics assemblies in spacecraft will be protected and not subjected to direct ATOX impingement, however, ATOX should be considered a constituent of the environment of the vented spacecraft, if only nominally.

2.5 UV Radiation

In the LEO environment, the energy of UV radiation is large enough to make modifications to the molecular structure of polymers. The UV radiation can break polymers bonds such as C–C, C–O and functional groups. It can also cause scissioning, create volatile fragments, or induce crosslinking. As a result, polymer properties (mechanical, thermal or optical) can be modified by the UV radiation. UV radiation may also act synergistically with ATOX, accelerating polymer property modification. Like ATOX, polymers used in spacecraft electronics are generally expected to be well protected from and not subjected to direct UV radiation exposure. Unlike ATOX, which may still interact with materials inside the vented spacecraft, it is highly unlikely UV radiation will indirectly interact with the polymers of interest in this study in most spacecraft electronics configurations.

2.6 Potential Reliability Issues of Underfill Associated with the LEO Environment

As explained previously, most commercial underfilled flip chip assemblies are non-hermetic. While Xilinx has fortified the space version of the V4 relative to the commercial version, the space version remains non-hermetic. As a consequence, the LP2 underfill material used in the V4 is exposed to and must be expected to interact with the spacecraft environment. For LEO missions the LP2 is tasked with protecting the flip chip interconnects in the environment described above.

The bond energy of the covalent carbon-carbon bond, the primary bond in organic polymers, is a relatively weak 80 to 90 kcal (335 to 337 kJ). Energy impulses into the polymer greater than the bond energy can break single bonds, creating two electron deficient molecules, or radicals, from the single chain. These molecules may recombine or move in separate directions and remain separated. Thermo-mechanical stresses can be sufficient sources of energy for this molecular cleaving. The energy introduced to the system increases with increasing temperature. The vacuum of space provides the driving force for diffusion and outgassing of low molecular weight fragments, additives, and adsorbed gasses from polymers used in spacecraft assemblies, including electronic assemblies and components. Coupled together, thermo-mechanical stresses on polymers under vacuum in LEO may experience increased degradation rates than in terrestrial conditions.

The effects of radiation on a polymeric material strongly depends on the molecular structure of the material, which is related to the presence of tertiary carbon, quaternary carbon, oxygen, chlorine, sulfur, and other additives. Radiation can induce crosslinking or scissioning. Both may take place at the same time, but often one is predominant depending on the molecular structure. Aromatic rings in a polymer's backbone structure have a radiation stabilizing effect on the polymer. Compared to other polymeric materials cured epoxies are more radiation resistant due to the presence of aromatic rings in the backbone structure, especially at low radiation doses [13]. Still, the amount of crosslinking and scissioning may be large enough to alter the bulk properties of cured epoxies. The resulting changes are to the elastic modulus and glass transition temperature [14]. Additionally, in nominally cured epoxies unreacted epoxide groups may exist. This occurs because the epoxy system vitrifies during cure, thus preventing additional reaction. The unreacted epoxide groups can undergo further reaction during radiation exposure resulting in changes to Tg, dynamic modulus, and loss tangent.

Overall degradation behavior of an epoxy by radiation exposure depends not only on chemistry but also radiation dosage. For example, in some epoxies, chain scissioning is more dominant than crosslinking at the early stage of radiation. The chain scissioning will result in decreased tensile strength and adhesion. However, as radiation exposure progresses, crosslinking can become more dominant and result in recovery of the mechanical properties [14].

It is difficult to predict the effect of radiation on LP2 underfill without carrying out systematic experiments. This is primarily because radiation can induce both improvement in and degradation to the properties of polymers. For example, polymers may be processed by irradiation using an electron beam. The irradiation induces crosslinking in the polymer which may improve the mechanical, thermal,

chemical and/or other properties. Electron beam processing is also used to deliberately degrade polymers. For example, when bulk polytetrafluoroethylene (e.g., Teflon®) is treated by electron beam processing, chain scissioning takes place and the bulk Teflon eventually transforms into a powder.

Due to shielding practices, electronics within a spacecraft are exposed to less harsh conditions than outside of the spacecraft. Inside the spacecraft, electronics and polymers used in electronics assemblies will be subjected to floating ATOX, rather than directly impinging ATOX, although ionizing radiation may still be significant without targeted radiation shielding. UV radiation is expected to be insignificant since it cannot penetrate the shielding. Among all the constituents of the LEO environment, the long-term vacuum exposure would be the most realistic environmental concern for the LP2 underfill material used in the non-hermetic V4 package.

3.0 TECHNICAL APPROACH

3.1 Cross-Sectional Observation of V4

Prior to performing experiments on LP2 underfill used in the V4 assembly, the structure of the die/solder bump/substrate interface was evaluated in cross-section.

3.1.1 Filler Settling

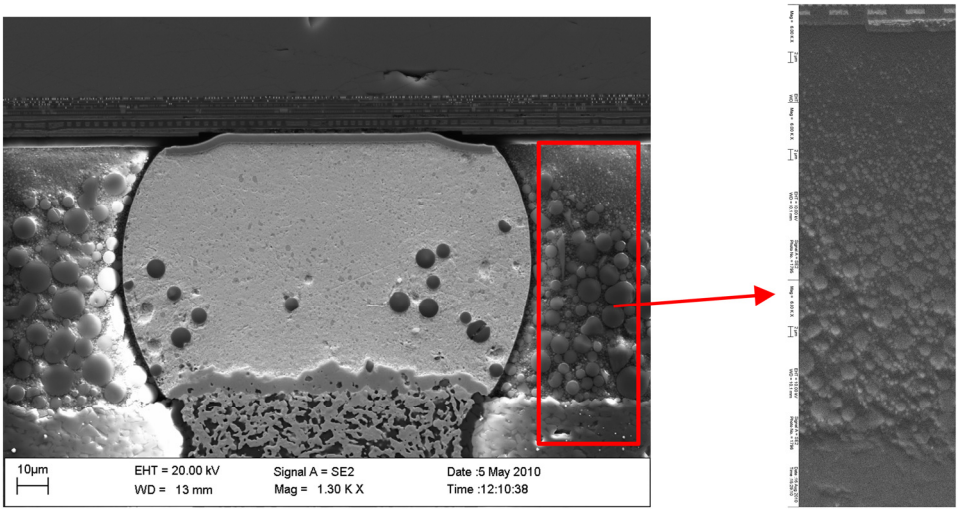

Figure 3-1. Filler settling of the LP2 underfill.

Figure 3-1 is a cross-sectional SEM image of a V4 flip chip solder bump. Some filler particles can be seen embedded within the solder bump. These are artifacts produced during sample preparation. Filler settling, characterized by filler particles concentrated at the substrate side, is noticeable. As a result, the die side of the underfill is left richer with soft resin, while the substrate side has a greater concentration of large filler particles. Larger filler particles settle due to gravity and create a gradient from the chip surface to the substrate surface. Filler settling occurs when uncured underfill does not have a viscosity high enough to hold the filler in suspension. This takes place if the base chemistry is not able to keep the filler buoyant or the temperature of the underfill is raised beyond the recommended flow temperature during the manufacturing process [15].

Settling of filler particles in underfill materials is a known issue and is generally considered undesirable. The filler-rich region is expected to be stiffer and stronger, while the resin-rich region is more compliant and weaker. The filler material is silica (SiO_2). The silica-rich region has a lower CTE and the resin-rich region has higher CTE. CTE of the LP2 underfill measured at JPL was 21.27 ppm/°C. CTEs of the resin-rich region and filler-rich region were estimated by measuring total area of filler and resin on both sides. The estimated CTEs were 13 ppm/°C and 26 ppm/°C at the filler-rich and resin-rich regions, respectively. From a pure CTE matching perspective, the opposite condition—the silica-rich region at the die side and resin-rich region at the substrate side, would seem desirable. The effect of underfill settling on the reliability of a flip chip package, however, is not clear at this point. Studies show opposing results. One study indicates that settling of silica particles has little effect on stress in solder and has only a minimum impact on the reliability of the solder bumps [16], while another study says that settling can lead to a reduction in the number of thermal cycles to failure by 50% [17].

Regardless of the disagreement in the literature, filler settling can affect adhesion. Excess filler at the bond surface will reduce adhesion as it decreases the available adhesive bond area at the interface. The filler-rich interface has been shown to have ~30% lower adhesion strength than the resin-rich interface

[18]. The authors attribute this to increased plastic deformation in the resin-rich region of the underfill. One might consider this to be an extension of the bond area or bond volume effect, as the ductility of the filler-rich region is significantly smaller than the resin-rich region do to the rigidity of the silica filler and the smaller concentration of the more ductile polymer. The overall effect of underfill settling on adhesion will also depend on the chemistry of the underfill [19].

3.1.2 Solder Joint Structure

The main purpose of the underfill is to ensure survivability of flip chip solder joints. Therefore, structure of the V4 flip chip solder joint will be briefly discussed.

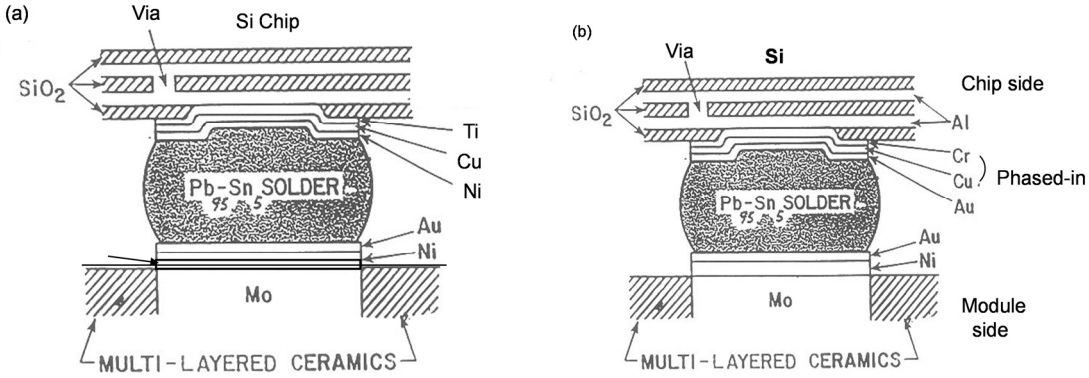

Figure 3-2. (a) Structure of the flip chip solder joint based on cross-sectional analysis and (b) the original IBM C4 solder joint structure

Figure 3-2 (a) is a schematic diagram of the V4 flip chip solder bump structure constructed based on cross-sectional analysis of the V4. Pb95Sn5 is the composition of the solder. Historically, in the IBM C4 process, 95Pb5Sn solder was used on an under bump metallurgy (UBM) consisting of Cr/phased-in Cu-Cr/Cu/Au. Pb95Sn5 solder was deposited on the UBM by evaporation, as shown in Figure 3-2 (b). Cr acts as an adhesion layer to adhere the Cu to the SiO_2 on the chip. Cu is the wetting layer and reacts with and bonds the solder. In order to enhance adhesion between Cu and Cr, Cu and Cr have a phased-in structure. Cu and Cr are co-deposited in a way that causes their grains to interlock. Au is a passivation layer, and a very thin layer (~300Å) of Au is used to prevent oxidation or contamination of Cu until the subsequent solder bumping process. This structure was developed more than 40 years ago and has been proven extremely reliable.

Later in the 1990s, the evaporated 95Pb5Sn was replaced with electroplated 97Pb3Sn and UBM was slightly modified to TiW/phased-in Cu-Cr/Cu. The main purpose of the change was to enable processing with larger wafers rather than to enhance the reliability. As the industry moved toward using organic substrates for low-cost applications, eutectic SnPb solder was introduced for organic substrates because organic substrates cannot withstand the high reflow temperature of high-Pb solders. The UBM structure originally developed for high-Pb solders could not withstand multiple reflows with eutectic SnPb. One solution was to use Al/Ni(V)/Cu/Au. Even though this structure was reliable when used with eutectic SnPb, it could not withstand multiple reflows with Pb-free solders.

IBM's solution for Pb-free application developed in the mid-2000s was to use TiW/phased-in Cu-Cr/Cu/Ni. Ni was electroplated and TiW/Cu-Cr/Cu layers were sputtered [20]. Intel has been using copper pillar bumps with very thin solder since the mid-2000s. The main purpose was to reduce the thermal stress. The added benefits were enhancement in electromigration reliability and elimination of the dewetting problem, which is due to dissolution of the UBM wetting layer into molten solder.

Even though V4 is packaged at IBM, flip chip solder bumping is not done at IBM. The UBM construction of the V4 is not common since it pairs Ni with high-Pb solder. The V4 UBM structure resembles that of typical low-cost flip chip solder bump for Pb-free solders. It is not clear why the UBM process developed for Pb-free solders is used with Pb95Sn5 solder. One possible explanation is decreased manufacturing cost achieved by sharing the UBM construction with the commercial Pb-free version of the V4, which uses an organic substrate.

The UBM for Pb-free solder should be able withstand multiple reflows with high-Pb solder, but long-term reliability of such flip chip solder joints are not known yet due to lack of existing studies. The aforementioned Cr- and Cu-based UBM developed by IBM has been used in mainframe computers for almost 50 years without issues. Therefore it has proved its reliability over a long timeframe, at least under terrestrial conditions. Ni was one of the candidates for UBM wetting layer material when IBM first developed their flip chip technology back in 1960s. Some of known reasons why Cu was selected over Ni are that evaporated Cu had lower stress and better wettability with high-Pb solder, providing better manufacturability. But it is not clear whether there were studies regarding long-term reliabilities of Ni UBM bonded to high-Pb solder. There is not much literature on the reliability of high-Pb flip chip solder joints as a function of UBM material, while data on eutectic or Pb-free solders are abundant. This is because high-Pb flip chip solder joints have been mainly used for mainframe computers and not widely used for consumer electronics applications. There is a study indicating that Ni is potentially incompatible with high-Pb solders [21]. But the use of Ni at the chip side may be acceptable as long as stress and wettability issues are resolved during manufacturing, because Ni has been used at the ceramic substrate side with high-Pb solder without any known issues. However, considering that space applications require higher reliability than commercial applications, lack of existing data indicates that there is a potential risk of having unknown long-term reliability of V4 flip chip solder joints.

3.2 Properties and Behavior of LP2 Underfill Material

3.2.1 Thermal Analysis Results

Tg, CTE, thermal degradation, storage modulus, and loss modulus are all fundamental properties of the LP2 underfill material that was investigated by Thermogravimetric Analysis (TGA), Differential Scanning Calorimetry (DSC), Thermomechanical Analysis (TMA), and Dynamic Mechanical Analysis (DMA).

3.2.1.1 Thermal degradation measured by thermogravimetric analysis (TGA)

Thermogravimetric analysis (TGA) measures changes in weight of a sample in relation to temperature. TGA can determine degradation temperatures. A cured LP2 material was crushed and went through TGA. TGA was carried out using a TA Q500 TGA instrument configured in the standard mode. The sample was heated to 750°C from room temperature at a ramp rate of 10°C/min. The sample compartment was purged with GN2. The resulting thermogram is shown in Figure 3-3. The weight loss profile indicated the onset of a weight loss transition at 373.94°C. This temperature later served as a reference in determining the upper bound of test conditions for DSC, TMA, and DMA tests. The LP2 retained nearly 70% of the original starting weight, even at temperatures approaching 750°C. Other epoxy materials with similar temperature of onset of weight loss generally show approximately 15% of the original sample weight remaining at 500°C. Hence it may seem that LP2 has very high capability of retaining its original weight compared to other epoxy materials. However, since LP2 is filled with a large amount of silica filler particles, the retention of weight is simply due to quantity of silica particles that remain after epoxy materials experience thermal degradation.

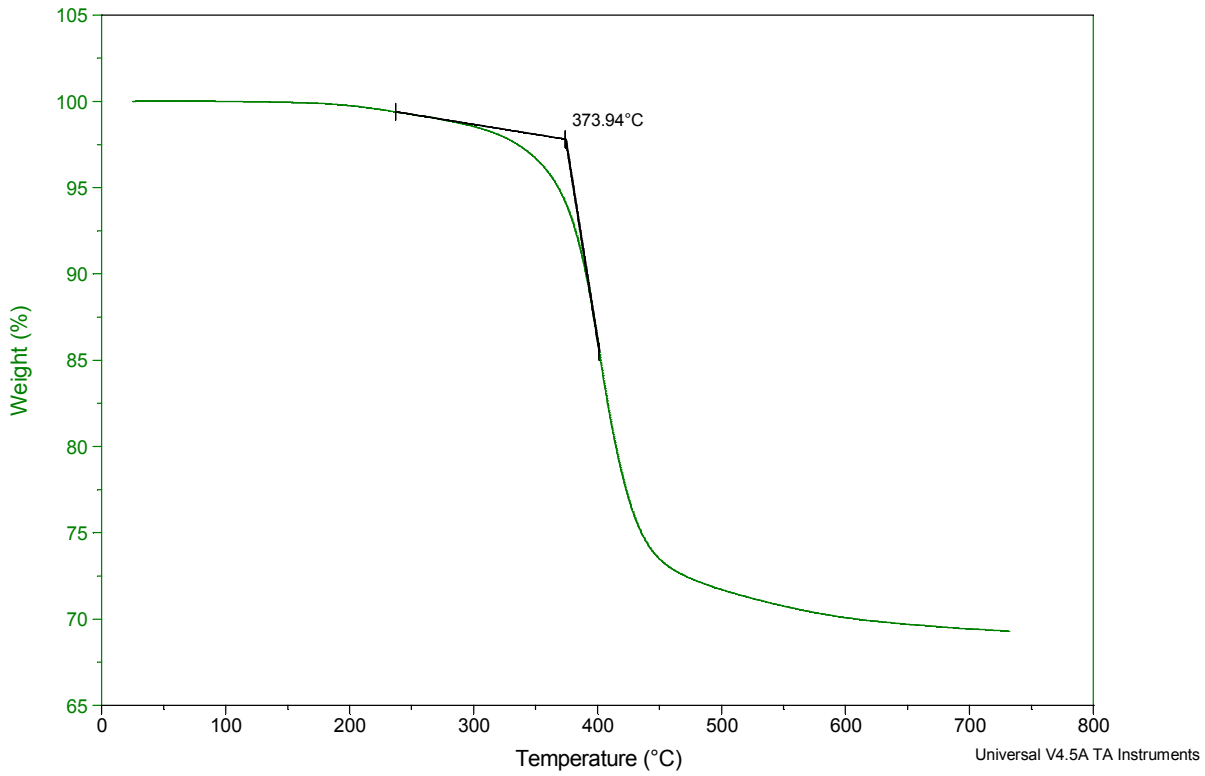

Figure 3-3. TGA result of the LP2 underfill.

3.2.1.2 Tg and residual cure measured by differential scanning calorimetry (DSC)

Since properties of a polymer material (i.e, CTE, elastic modulus, electrical impedance) dramatically change at glass transition temperature (Tg), it is desirable for underfill materials to have Tg outside the operating temperature range of the package. The LP2 underfill material has two different cure schedules. The recommended cure schedule has higher cure temperature and shorter cure time. Unlike the temperature at the onset of thermal degradation, Tg, CTE, and residual cure are rather sensitive to cure schedule. Therefore, samples with each cure schedule were made. Tg and residual cure was measured with differential scanning calorimetry (DSC). The DSC technique measures amount of heat required to increase the temperature of a sample as a function of temperature. DSC can measure Tg and the residual cure of a polymeric material. DSC was carried out using a TA Q100 DSC instrument configured in Standard DSC mode using a Refrigerated Cooling System (RCS) accessory. LP2 samples were equilibrated at a temperature well below –50 ºC, held isothermal for 5 minutes, and heated to a temperature well above +180 ºC at 5 ºC/min while purging the DSC compartment with GN2.

Figure 3-4 shows the DSC thermogram of LP2 material. The Tg of the sample cured with the recommended cure schedule was in between +125 and +190°C. However, Tg of the sample cured with the alternative cure schedule was several tens of °C below +125°C. Residual cure of the sample cured with recommended cure schedule, however, was larger than the residual cure of the sample cured with the alternative cure schedule.

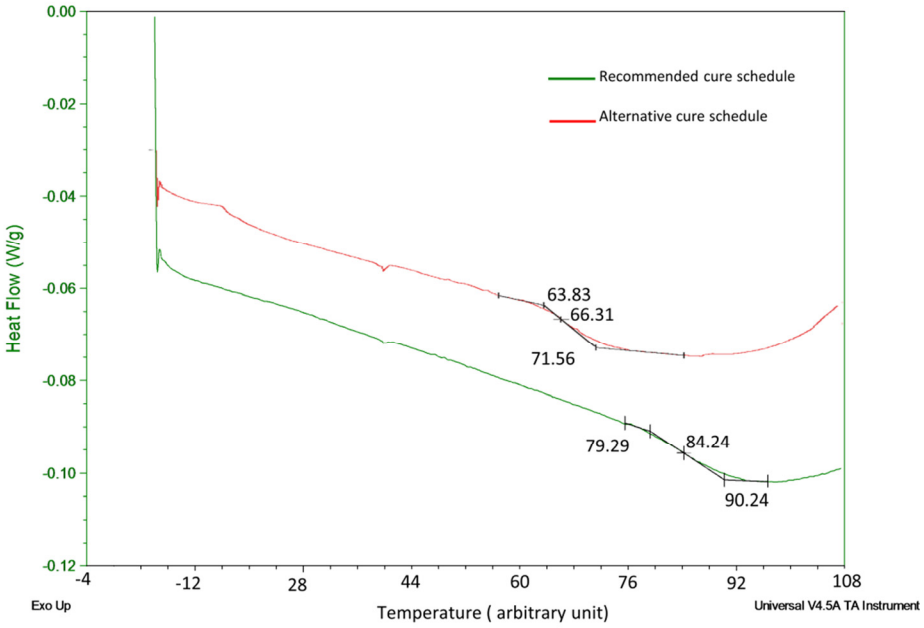

Figure 3-4. DSC test result of LP2 underfill material.

3.2.1.3 Tg and CTE measured by thermomechanical analysis (TMA)

Thermomechanical analysis (TMA) measures dimensional change of a sample as function of temperature. TMA can be applied to measure various properties of a material. In the current study, Tg and CTE of the LP2 materials were measured with TMA. TMA was performed on cylindrical LP2 samples, one cured under the recommended cure schedule and the other one cured under the alternative cure schedule. TMA was carried out using a TA Q400 TMA instrument configured in standard mode with an expansion probe using a probe force of 0.020 N. Both diameter and height of LP2 samples were about 2 mm. The sample was equilibrated at a temperature between –150 and –100ºC and held isothermally for 5 minutes. Then the sample was heated to a temperature well above 200ºC at 5ºC/min ramp rate. The TMA sample compartment was purged throughout the run using GN2. The resulting thermogram is shown in Figure 3-5. Two approximately linear regions of differing rates of thermal expansion were observed. The sample cured with the recommended cure schedule had a CTE of 21.27 ppm/°C below a temperature between 20 and 70°C. At temperatures above the range of 120 to 200°C, CTE was 75.46 ppm/°C. The CTE was found to be nonlinear in the intermediate temperature range between the two linear regions mentioned above. Even though the non-linear region lies within normal usage temperature of the V4 package, close examination of the TMA thermogram showed that CTE of the LP2 underfill cured with the recommended cure schedule does not deviate greatly from ~25 ppm/°C up to 125°C. Since thermal aging slightly changes properties of LP2 underfill (which will be discussed later), it will be also necessary to investigate how much the TMA test result will change after thermal aging in the FY12 task. For the sample cured with the alternative cure schedule, CTE was 19.33 ppm/°C at a temperature between 30 and 90°C, and 66.38 ppm/°C above a temperature between 70 and 120°C. Extrapolation between the two linear regions provides a Tg value determined by TMA. The measured Tg values were similar to DSC results. The Tg of the sample cured at the recommended cure schedule was well above +125°C, while samples cured at the alternative cure schedule were lower than +125°C. The sample cured at alternative cure schedule not only had Tg lower than 125°C but also had 66.38 ppm/°C of high CTE at 125°C.

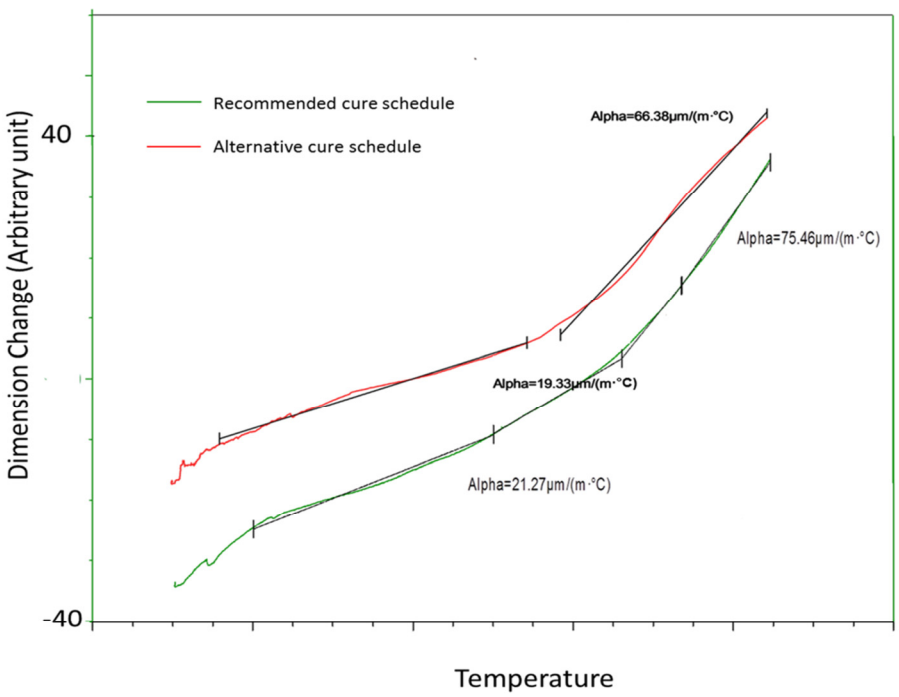

Figure 3-5. Thermogram of TMA test results on LP2 samples.

3.2.1.4 Dynamic mechanical analysis (DMA) results

Dynamic mechanical analysis (DMA) is a dynamic method of characterizing the viscoelastic properties of a material. A sinusoidal force (stress) is applied to the material at a set frequency and the response (strain) to this input is measured. The ratio of peak stress to peak strain gives a complex modulus from which storage modulus (G') and loss modulus (G") are obtained. The storage modulus is related to the energy stored by the material per cycle. An example storage modulus curve is presented in Figure 3-6.

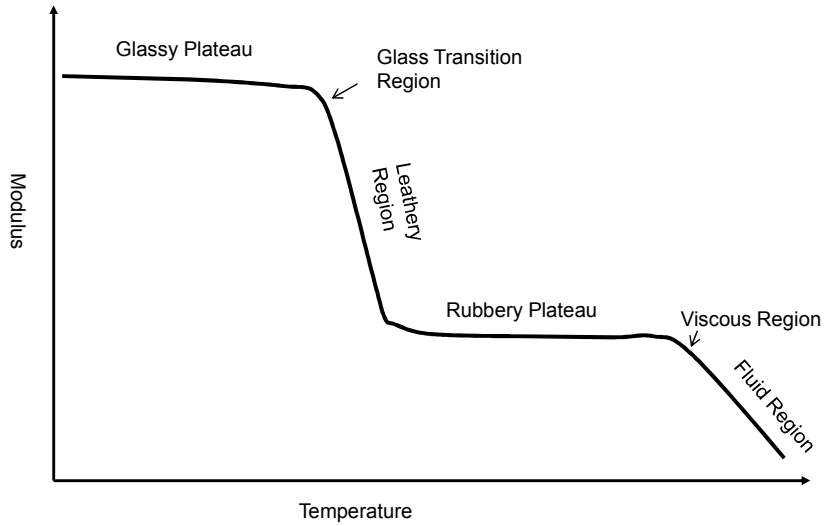

Figure 3-6. Typical storage modulus curve from viscoelastic regions of polymers.

Stiff and "glassy" materials have a high storage modulus. The loss modulus is related to the energy dissipated or lost by the material during the cycle and it will go through a maximum value during the glass transition region of the sample. Tangent Delta (tan δ) is the ratio of the loss modulus to the storage modulus (G"/G') and is commonly referred to as the loss factor. Tangent Delta is related to the viscoelasticity and damping (how well the material can disperse energy) of a material. The maximum in the tan δ peak is commonly labeled as the glass transition temperature (Tg).

DMA was performed on a TA Q800 DMA instrument configured in a single cantilever mode and a gas cooling accessory (GCA) and run from a temperature several tens of degrees below –100ºC to a temperature several tens of degrees above +150ºC with a ramp rate of 2ºC/min, at a constant frequency (1 Hz) and constant amplitude (20 μm). The dimension of LP2 samples was 40×10×2 mm. In Figure 3-7, the storage and loss moduli and tan δ are plotted. For the sample cured at the recommended cure schedule, it was found that the onset of storage modulus drop occurred at temperature several °C below +125°C, the peak maximum of the loss modulus and tan delta were both several tens of °C above +125°C. For the sample cured at alternative cure schedule, all the temperatures above dropped by roughly 20 to 50°C.

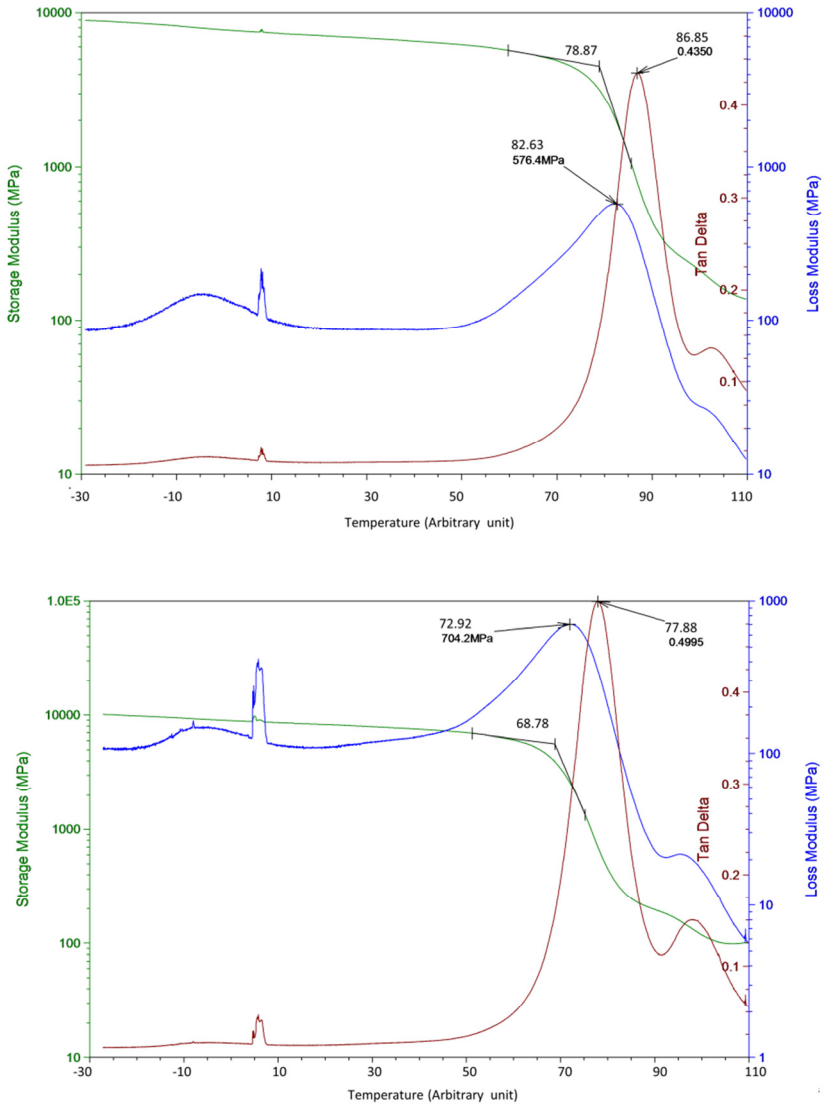

Figure 3-7. DMA test result of the LP2 underfill material cured at (top) recommended cure schedule and (bottom) alternative cure schedule.

3.2.2 Mechanical Properties of LP2 Underfill Material

3.2.2.1 Mechanical properties of LP2 underfill material measured by nanoindentation

The elastic modulus of the underfill is an important property. It should be large enough to carry the stress from the solder bumps without exerting excessive stress on the die. The elastic modulus of the underfill is also important when identifying the level of stress or stress distribution that flip chip solder bumps will experience. The stress distribution or amount of stress can be measured by Moiré interferometry [22] or Synchrotron micro-x-ray diffraction [23]. The most frequently used method among flip chip manufacturers, however, is to conduct finite element analysis (FEA) [24]. In future missions, packaging engineers at NASA may need to conduct FEA on V4 packages. Since electronic assemblies in a spacecraft are exposed to a wide range of temperatures, it is also necessary to know the mechanical properties of the underfill over a similar temperature range.

Young's modulus (E) and hardness (H) were measured by nanoindentation. The nanoindentation testing was performed using a MTS Nano Indenter XP instrument installed with a diamond Berkovich indenter, with strain rate of 0.05 /sec. Hardness and Young's modulus were calculated using the method by Oliver and Pharr [25]. Figure 3-8 is a load-displacement curve of a bulk LP2 underfill sample. Average Young's modulus and average hardness of samples cured at the recommended cure schedule were 8.9 GPa and 0.52 GPa, respectively (8.9 GPa of Young's modulus is high enough to transmit stress to the substrate and reduce strain on the solder joints [6]). Samples cured at the alternative cure schedule had lower Young's modulus and hardness than samples cured at recommended cure schedule, as shown in the Table 3-1.

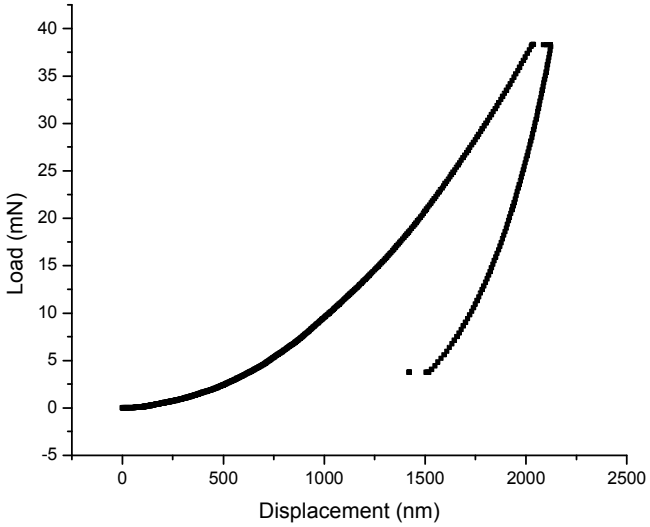

Figure 3-8. A nanoindentation load-displacement curve of a bulk LP2 underfill material.

Table 3-1. Young's modulus and hardness of LP2 underfill materials.

Cure Schedule	Young's Modulus (GPa)	Hardness (GPa)
Recommended cure schedule	8.9	0.52
Alternative cure schedule	4.6	0.32

3.2.2.2 Effect of thermal aging on mechanical properties of the LP2 underfill

An LP2 sample cured with the recommended cure schedule was thermally aged at 125°C up to 4 weeks to investigate effect of thermal aging on mechanical properties. Figure 3-9 shows load-displacement curves of LP2 samples thermally aged for different time.

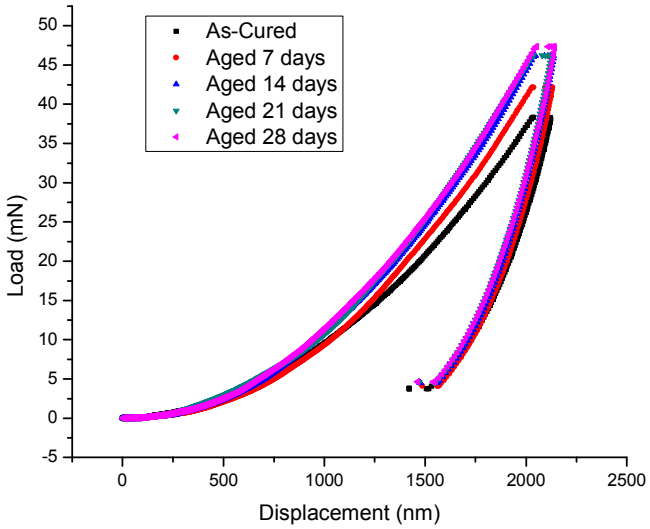

Figure 3-9. Nanoindentation load-displacement curves of LP2 underfill samples with different thermal aging history.

Table 3-2. Young's modulus and hardness of thermally aged LP2 material measured by nanoindentation.

Aging Time (days)	Average Young's modulus (GPa)	Average Hardness (GPa)
0	8.896	0.515
7	9.875	0.56
14	10.822	0.652
21	10.782	0.634
28	10.777	0.637

Table 3-2 shows changes in Young's modulus and hardness of LP2 underfill as a function of duration of the thermal aging. Both properties increased and reached plateau within 14 days. This indicates that changes in mechanical properties by additional cross-linking from thermal aging can be completed in less than 14 days at 125°C. This can serve as rough reference for future experiments involving thermal aging. In the current study, mechanical properties of the LP2 material were only investigated at room temperature. It would be necessary to perform additional tests at different temperatures in the future. It would be also necessary to investigate how long-term exposure to vacuum affects mechanical properties of the LP2 underfill. In FY12, effect of long term vacuum thermal aging on mechanical properties of LP2 underfill will be investigated, along with measurement of mechanical properties at different temperatures.

3.2.2.3 Adhesive strength of LP2 underfill material

As stated previously, adhesion is considered to be the most important property of the underfill with respect to enhancing reliability. An underfill needs to maintain good adhesion to the die, solder bumps and substrate. The lifetime of a flip chip package is expected to drop 50% to 75% when delamination occurs at any place in the module. Adhesion of underfill to solder bumps is also important. A simulation study indicates that, even though delamination from the chip/ substrate interface results in a significant increase in stress, delamination from solder joints can induce accumulated inelastic shear strain on those solder joints, which can be more damaging [17]. Most failures occur with the onset of delamination at interfaces. Hence, an underfill's ability to retain interfacial adhesion after exposure to adverse conditions

is critical to the reliability of the flip chip package. For example, the pressure cooker test (PCT) involves adhesion testing after exposing the underfill to 100 percent relative humidity at 121°C and 15 psi pressure [15, 26].

There are several adhesion test methods for underfill used in commercial industry. One method is to bond the die to the substrate using the underfill and perform a die shear, lap shear, or stud pull test. The test is conducted at various temperatures. However, silicon is brittle and breaks in unpredictable ways, which strongly affects the distribution of experimental values [27]. Therefore, direct determination of the adhesion strength of the underfill layer to the silicon passivation is considered to be a very difficult task. The current draft of IPC standard J-STD-030 recommends performing lap shear tests along with die shear and stud pull tests for comparative estimations. The use of ASTM standard D1002 is recommended for lap shear testing. Underfill manufacturers also frequently perform lap shear tests based on the ISO 4587 standard. In the current study, lap shear tests were done according to ASTM D1002. Two aluminum plates were bonded with the LP2 underfill without primer. Figure 3-10 shows the dimensions of the lap shear test specimen. The thickness of the LP2 underfill is controlled by using two 5-mil stainless steel wires as spacers.

Since the package will be exposed to wide range of temperatures during an actual mission, lap shear strength was measured at +125°C, +22°C, and –55°C. Lap shear tests were done on 5 lap shear samples per each temperature condition. Test results are as shown in Tables 3-3 to 3-5. All the samples exhibited adhesive failure. Figure 3-11 shows how lap shear strength of LP2 underfill changes according to temperature. At room temperature, average strength was 3043 psi. The lap shear strength decreased as temperature increased. The average lap shear strength at +125°C was 2405 psi, which is still high enough for underfill applications. This indicates adhesive strength of LP2 underfill material remains very high throughout common usage temperatures.

Even though the current study was performed at temperatures relevant to conditions in space, it would also be necessary to investigate changes in adhesive strength of the LP2 underfill after exposure to relevant LEO environment conditions. In FY12, the effect of long-term exposure to vacuum thermal aging on lap shear strength will be investigated.

Table 3-3. Lap shear test results of the LP2 underfill material.

Sample	Length (in)	Width (in)
1	0.498	0.994
2	0.4935	0.9975
3	0.4945	0.9995
4	0.4915	1
5	0.4855	1

Table 3-4. Lap shear test results of LP2 underfill material at +125°C. The average lap shear strength is 2405 psi.

Sample	Length (in)	Width (in)
1	0.490	0.999
2	0.491	1.000
3	0.493	0.997
4	0.488	0.995
5	0.492	1.000

Table 3-5. Lap shear strength of LP2 underfill material at -55°C. The average lap shear strength is 3228 psi.

Sample	Length (in)	Width (in)
1	0.4875	1.0000
2	0.4885	0.9975
3	0.4970	0.9970
4	0.4940	0.9970
5	0.4860	0.9985

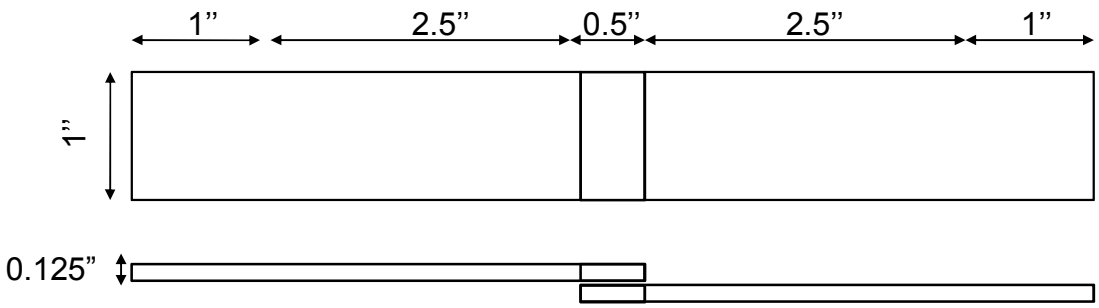

Figure 3-10. Dimension of lap shear test specimen.

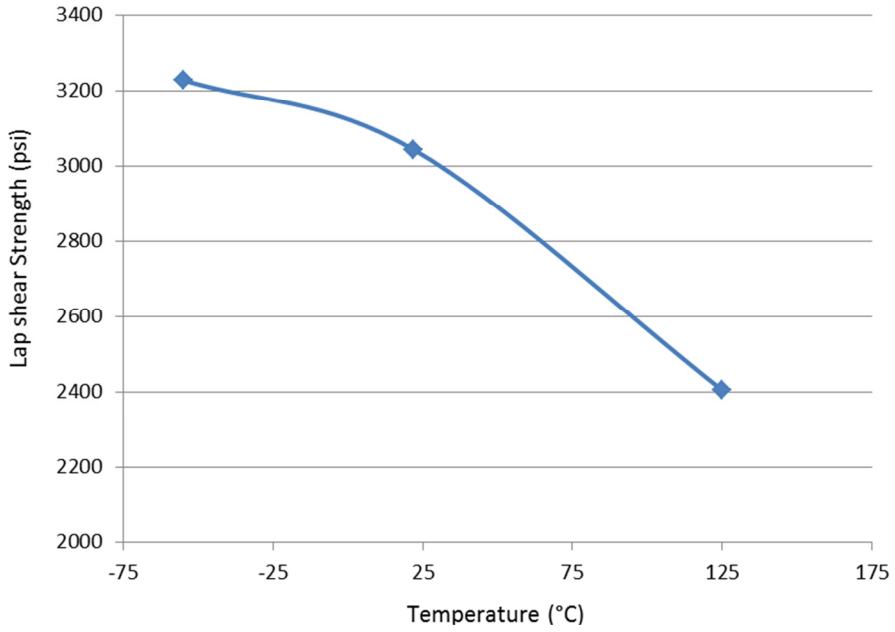

Figure 3-11. Change of lap shear strength as a function of temperature.

3.2.3 Outgassing Behavior of the LP2 Underfill

Due to the non-hermeticity of the V4, the underfill material is directly exposed to high vacuum, making outgassing of the underfill material a concern. In terms of manufacturing, a good underfill should have low outgassing during the cure in order to prevent void formation. Hence an underfill is often formulated to have a low amount of volatile components that can outgass during cure, which may also reduce

outgassing at high vacuum. According to outgassing measurements by Xilinx in 2006, the level of outgassing was acceptable and met NASA requirements for total mass loss (TML) and collectable volatile condensable material (CVCM). The CVCM result from Xilinx indicated that outgassing of the LP2 underfill is similar to common aerospace grade epoxies. However, the effects of the LEO environment were not considered in those measurements. In the current study, only the effect of vacuum thermal cycling and radiation on outgassing of LP2 underfill were investigated. In addition, the outgassing rate was also investigated at the Molecular Contamination Investigation Facility (MCIF) at JPL.

3.2.3.1 Effect of vacuum thermal cycling

Polymer chain fragmentation from vacuum thermal cycling can generate volatile components inducing further outgassing. Additional surface area resulting from cracking or crazing of a polymer can increase outgassing rates. V4 packages were polished to expose solder bumps and underfill, as shown in Figure 3-12. In some samples, the underfill was pre-cracked. The samples were installed in a thermal cycling vacuum chamber along with witness plates. The samples were thermal cycled from –55 to +125°C. Samples were thermal cycled up to 133 cycles for 33 days. The low volatility residue (LVR) was analyzed using Diffuse Reflectance Infrared Fourier Transform (DRIFT) spectroscopy [28]. Blank samples were run along with the samples. FTIR provides chemical functional group information for quantitative analysis and qualitative identification of materials. The analysis followed the JPL ACL-120 procedure that complies with IEST-STD-CC1246D.Table 3-6 shows chemical analysis results from up to 30 cycles, and the amount of the detected component was very low. According to the FTIR spectrum most of detected components were from vacuum pump oil. There was no indication of detectable amounts of outgassing from epoxy (underfill).

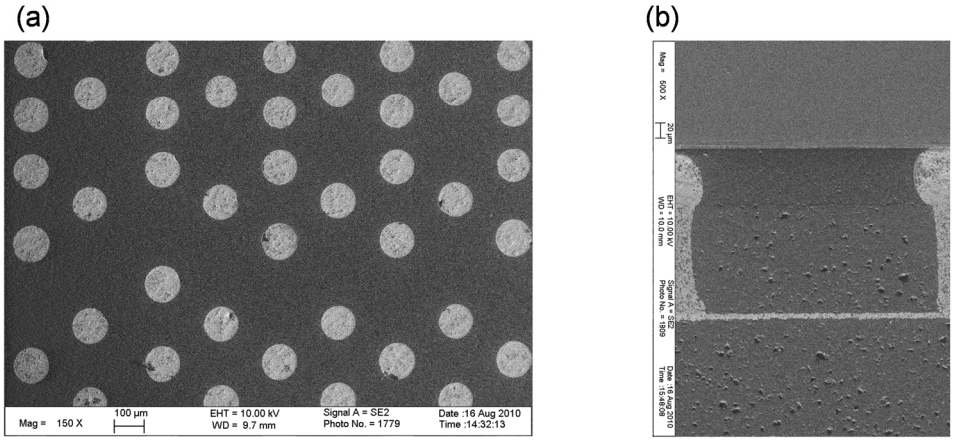

Figure 3-12. V4 samples for vacuum thermal cycling: (a) top-view sample (b) cross-sectional sample.

Table 3-6. Lap shear strength of LP2 underfill material at –55°C. The average lap shear strength is 3228 psi.

Sample	Chemical Functional Group	Amount (µg/cm²)
Post bake (125°C for 24 hrs)	Aliphatic hydrocarbon	0.06
10 cycles	Aliphatic hydrocarbon	0.04
30 cycles	Aliphatic hydrocarbon	0.08

3.2.3.2 *Effect of radiation on outgassing*

Radiation can induce scissioning and generate volatile fragments, resulting in additional outgassing. Radiation effects on the outgassing of the LP-2 underfill were investigated using DMA-type bulk LP2 samples. Ideally, radiation dosing would be performed using precisely controlled irradiation apparatus such that the exact value of radiation energy and dosage is known. In the current study, however, the operational space with respect to LEO radiation is being investigated to determine if there is a measureable effect on outgassing of underfill. Therefore, an RF plasma machine was used for dosing purposes instead of the standard irradiation apparatus. The radiation species is a mixture of charged ions, electrons and atomic oxygen.

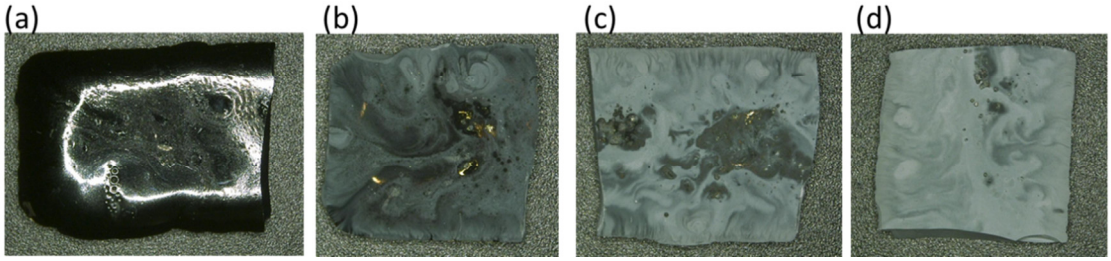

Figure 3-13. Erosion of LP2 underfill after (a) 0 hr (b) 2 hr (c) 4 hr and (d) 6 hr of exposure to O_2 plasma.

After exposure to the O_2 plasma, the originally dark surface of LP2 underfill was eroded to white surface, exposing particles of SiO_2 fillers, as shown in Figure 3-13. In order to investigate whether exposure to O_2 plasma has created any volatile components, one as-cured sample and one sample treated with 6 hours of O_2 plasma were analyzed with Direct Analysis in Real Time (DART). DART is a non-vacuum test. It uses metastable helium to dissolve a material and then mass spectroscopy is done on the metastable helium. It can provide the molecular weight distribution of volatile components.

The DART method can serve as a low-cost alternative for CVCM test, by assessing the outgassing potential relative to reference polyethylene material with a known, nominal vacuum condensable material (CVCM) level. The plasma treated and untreated LP2 coupons were extracted with dichloromethane (DCM) for 1 hour. This solvent dissolves a wide range of vacuum outgassing products at the material surface. It can also penetrate through the layer of SiO_2 particles on the sample treated with O_2 plasma and dissolve outgassing products. The extracted residues in DCM were then analyzed using the DART sampling system coupled to a high mass accuracy, time of flight Mass Spectrometer (DART-AccuTOF). The DART-AccuTOF system uses meta-stable helium as a surface ionization source that is temperature controlled. This enables molecules that are otherwise difficult to ionize and volatilize to be readily introduced into the mass spectrometer system. The system measures the parent ion of the molecule (M and/or M+1) with an accurate molecular weight of the desorbed compounds. This method determines the presence of vacuum labile residues from plasticizers, additives and uncured polymeric materials. The measurement is compared to a similarly processed standard polyethylene material with a known CVCM of 0.07%. The DART result showed that the plasma treated LP2 test coupon had a significantly lowered amount of residue in the 100–360 amu range compared to the untreated test coupon, as shown in Table 3-7. The 100-360 amu range is where most of the peaks were located for LP2 material, as shown in mass spectra in Figure 3-14. The plasma processing of the epoxy significantly reduced the vacuum labile residue to a level below that of the polyethylene standard, with a 0.07% CVCM. Therefore, it was concluded that the plasma treatment resulted in a removal of surface residues that were not cross-linked in the epoxy cure and etched into the epoxy surface, not creating any potential contaminant.

Table 3-7. DART-MS result of O_2 plasma treated and untreated LP2 material, with respect to reference polyethylene with known CVCM level.

Sample	Total Ion Current in the 100–360 amu Range
1. Untreated LP2	8 K
2. Plasma Treated LP2	0.1 K
3. Reference U.LO. PE	0.4 K

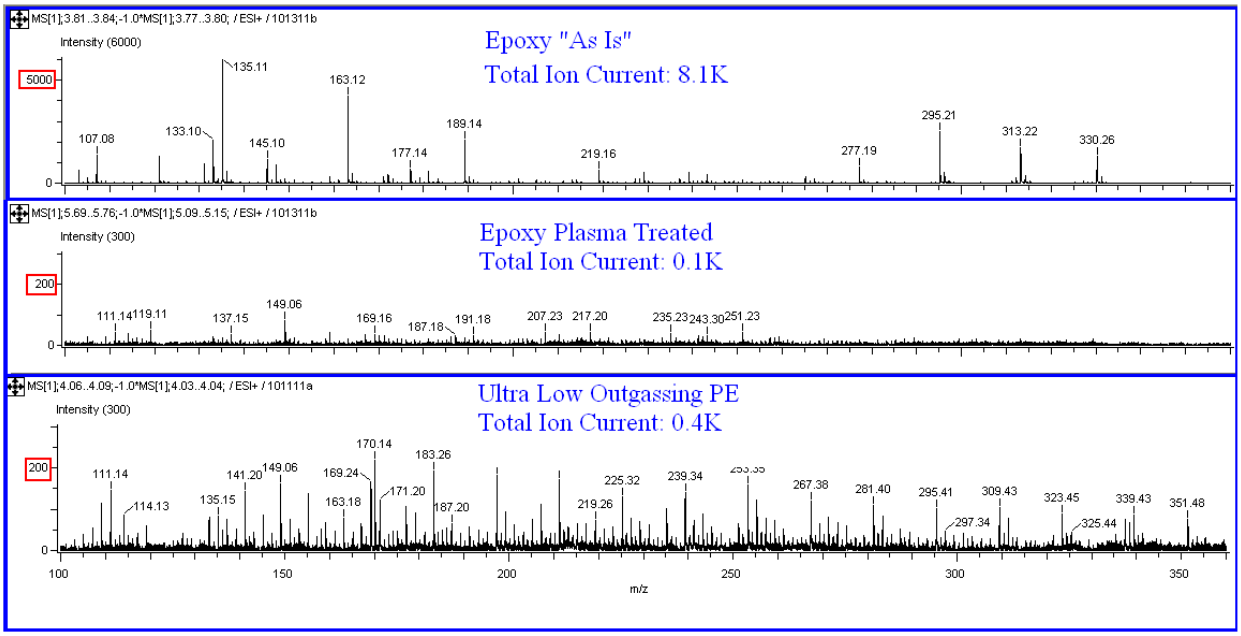

Figure 3-14. DART MS spectra showing as-cured LP2 has considerably more residue in the 100-350 amu range than plasma treated LP2 material. A spectra of ultra-low outgassing polyethylene is also shown as a reference.

3.2.3.3 Outgassing rate

Even though the LP2 material has passed CVCM test requirements, the outgassing rate and behavior of the LP2 underfill at vacuum merited further study. Outgassing rate of the LP2 underfill material was investigated at the Molecular Contamination Investigation Facility (MCIF) at JPL [29]. The main difference between the MCIF and CVCM tests is that MCIF is a kinetic test and CVCM is an accelerated test. In the CVCM test, a material is heated in vacuum beyond the ordinary usage temperature in order to quickly drive out volatile components. The CVCM test can provide the total amount of volatile component that can eventually outgas but not how fast volatile components will outgas. In the MCIF method, a sample is heated to different temperatures in vacuum and the target is cooled to different temperatures to collect volatile components. The MCIF has conducted an outgassing evaluation test on a 4.1-gram sample of LP2 underfill material. The objective of the test was to measure the outgassing rates of the LP2 underfill material at 20, 40, 60, 80, 100 and 110°C while continuously collecting data on both -50 and –20°C Quartz Crystal Microbalances (QCM). The test was conducted using the provided LP2 Underfill Material, which was placed in a perti dish, inside the Knudsen-cell (sample isolation chamber). Vacuum was established (10^{-5} Torr), two Quartz Crystal Microbalances (QCMs) were set at collection temperatures of –50°C and –20°C. The sample heat exchanger temperature was maintained at these temperatures for three days. Data was continuously collected measuring the molecular outgas levels, temperatures and pressure. Figure 3-15 shows the configuration of the MCIF chamber.

The chamber with the LP2 underfill material slowly pumped down to 10^{-5} Torr in 7 hours. Then the QCMs were cooled to their collection temperatures, while the sample heat exchanger was maintained at ambient then heated in steps up to 110°C. QCM data was continually collected throughout the test. Tables 3-8 and 3-9 show the QCM data. Since the witness plate experiment during vacuum thermal cycling showed almost no detectable amount of outgassing species, LP2 underfill was expected to have a low outgassing rate. The outgassing rate measured with MCIF was lower than what we expected. The LP2 Underfill material collection rates on the two QCMs were very low. The rates were similar to the empty chamber background levels achieved prior to testing LP2 material. MCIF results can also be used to estimate the outgassing rate of a material at a given temperature by performing tests on various temperatures. From the measured data, one can obtain rate constant and activation energy and then extrapolate to the temperature of interest. However, since the outgassing rate of the LP2 underfill was extremely low, there is no need to perform this calculation.

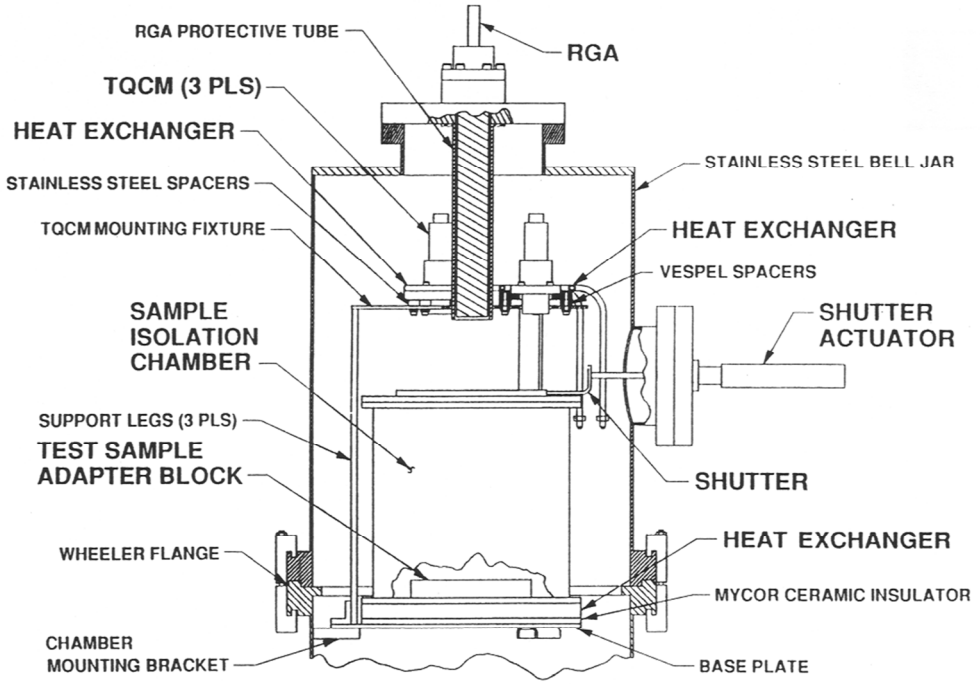

Figure 3-15. MCIF chamber configuration.

Table 3-8. –50°C Thermoelectric QCM collection results from the MCIF test.

Temperature °C	Total Accumulation Hz	Accumulation per Hour Hz/hr Avg.
20	3.50	1.17
40	2.30	1.15
60	4.70	0.34
80	2.50	0.42
100	7.10	0.44
110	2.30	0.38

Table 3-9. –20°C thermoelectric QCM collection.

Temperature °C	Total Accumulation Hz	Accumulation per Hour Hz/Hr Avg.
20	3.00	1.00
40	2.30	1.15
60	5.00	0.36
80	2.40	0.40
100	8.90	0.56
110	3.70	0.62

3.2.4 Volume Resistivity and the Effect of Radiation Charging on Underfill

There have been questions among some members of the space community, based on their experiences with printed circuit board encapsulation, as to whether or not there is any likelihood radiation may induce arcing of the underfill. Printed circuit board encapsulation can sometimes charge to a point where arcing occurs. This is due to the dielectric breakdown of the encapsulation. In order to minimize the risk of arcing, such dielectrics are recommended to have a minimum conductivity. If underfill shares the same concerns, it will potentially damage the adjacent metallization on the device. Any material that will hold onto the implanted charge from electrons or protons can present a danger unless that charge bleeds away fast enough to avoid dielectric discharges. If the LP2 material is resistive enough arcing could be a problem, but only if used improperly. Based on the structure of the V4 package, there are several mitigating factors for this issue. For a material to become charged, electrons or protons need to stop in the material, thus adding their charge to the neutral material. If enough charge stays in the material, large electric fields can be formed, which would lead to dielectric breakdown. In the case of very thin materials surrounded by thick materials, this generally does not happen since the energetic electrons or protons either are stopped by other materials before they reach the material or pass through it entirely. Since the LP2 material is used as an underfill, the thickness of the LP2 is very thin (about 100 μm). In addition, it is sandwiched between several thick layers of material (SiC lid, Si die, Alumina substrate, PCB board). Finally, the danger from a charged dielectric is related to the size of exposed area and the sensitivity of a nearby device (chip, circuit, etc.). If the area that is exposed is small enough, very little charging occurs and the amount of energy released by a discharge is extremely small and potentially insignificant. These are the reasons why arcing has never been a problem with SiO_2 dielectrics in the silicon device; for one, they are too thin and have too small an exposed area to cause a problem. When it comes to the LP2 underfill, the charged particles will either be trapped by other materials or pass through the LP2. Even if discharging takes place, the amount of energy will be extremely small. If the LP2 material were used as a potting material, where it would be both of greater thickness and more exposed to energetic electrons, it would likely be an issue. In such an application, the material would need to be resistive enough for the intended use, but also have minimum conductivity to bleed away charge fast enough that dangerously large electric fields never form.

Even though radiation charging seems to be a small concern based on the geometry of the package, it is important to understand the basic electrical properties of the LP2 underfill material. The lower bound of the resistivity of the LP2 material was measured with a standard resistivity cell. Uncured LP2 underfill material was spin-coated to N+ type 4-inch silicon wafer to produce a thickness of 75μm. Volume resistivity of the LP2 underfill material was measured by a HP 4329A high resistivity meter paired with a 16008A resistivity cell to measure resistivity. The average measured volume resistivity was 3.92×10^{15} ohm-cm. In general, radiation charging is only a concern for materials with resistivity over 10^{15} ohm-cm. Based on its high resistivity, radiation charging would be a concern if the LP2 underfill material was used for different purposes, such as a potting material. However, as discussed above, the risk of radiation charging is low when it is used as an underfill material, because the geometry of the package will prevent the LP2 underfill material from charging.

3.2.5 The Effects of the LEO Environment On Properties of LP2 Underfill Material (FY12)

In the current study, a series of tests were done to measure properties and to study the behavior of the LP2 underfill. However, most of tests were performed under atmospheric pressure and additional tests are required to verify long-term reliability of the LP2 underfill at LEO.

Long-term vacuum exposure is the most realistic and relevant LEO environment issue for the V4 package. Exposure to vacuum at an elevated temperature can also affect the properties of an epoxy. It is also necessary to investigate the effect of vacuum thermal aging and radiation on the elastic modulus and glass transition temperature of the underfill. In addition, lap shear strength tests will be needed on samples exposed to vacuum thermal aging for long periods of time. Even though radiation effects are of a lesser concern than exposure to vacuum, thermal analysis on LP2 underfill material treated with O_2 plasma would need to be performed. One reason is that unreacted epoxide groups can often exist in cured epoxies. This is due to vitrification during cure preventing additional reaction. The unreacted epoxide groups can then undergo further reaction when exposed to the radiation. Radiation can induce crosslinking or scissioning, which can result in changes in the elastic modulus and Tg of an epoxy [14]. The additional reaction can also result in dynamic modulus and loss tangent changes. Therefore, it would be necessary to run thermal analysis, such as DSC, TMA, and DMA on radiated samples of LP2. However, LP2 underfill samples treated with O_2 plasma are not suitable for TMA and DMA analysis. As shown previously, the surface erosion of LP2 underfill from O_2 plasma exposure changes the surface of an LP2 sample into a porous state, covered with powdery SiO_2 filler particle residues. This makes O_2 plasma treated samples not suitable for TMA and DMA analysis, because the porous and powdery surface will affect mechanical measurement in TMA and DMA analysis. In addition, ionized species created by the RF plasma machine may not be able to penetrate into the bulk of a sample and change properties of the LP2 material. If only the surface of the specimen is affected by radiation, changes in properties may not appear in TMA and DMA tests. DSC study can be done on the O_2 plasma treated LP2 material. DSC study of O_2 plasma treated samples will be done in the FY12 task.

In the current study, Young's modulus of the LP2 underfill was measured with nanoindentation. Mechanical properties of polymer material can also be measured with ASTM D638 type tensile test [30]. Nanoindentation was preferred over the tensile test in this case because nanoindentation did not require preparation of dog bone shaped samples. The limitation of using nanoindentation is that most nanoindentation machines cannot perform tests at different temperatures from +125°C to –55°C. This is due to difficulties installing hot/cold stages that do not cause vibration. In order to fully understand behavior of the LP2 material under temperatures relevant to space applications, Young's modulus of the LP2 material should be measured under different temperatures, using specimens constructed per ASTM D638. The dimension of the specimens will be as shown in Figure 3-16. If significant changes in mechanical properties are observed with nanoindentation on samples treated with vacuum thermal aging, tensile tests will also be done at different temperatures on samples treated with vacuum thermal aging.

Since V4 packaging is non-hermetic, the effect of processing fluids is also a concern. Due to the presence of high vacuum and highly sensitive sensors, spacecraft electronics have to be extremely clean after assembly. During assembly, the non-hermetic V4 will be exposed to a variety of processing fluids. If those fluids are absorbed into the LP2 underfill or are somehow trapped at the interfaces between the underfill and other materials and are not baked out or otherwise removed, they will outgass and potentially contaminate critical components, such as sensors, during the mission. To ensure that LP2 underfill is stable with regard to processing fluids, a V4 package or bulk LP2 sample will be exposed to various processing fluids using predicted assembly methods and conditions, then cleaned and baked out using expected practices. The samples will then be tested for outgassing with the DART method.

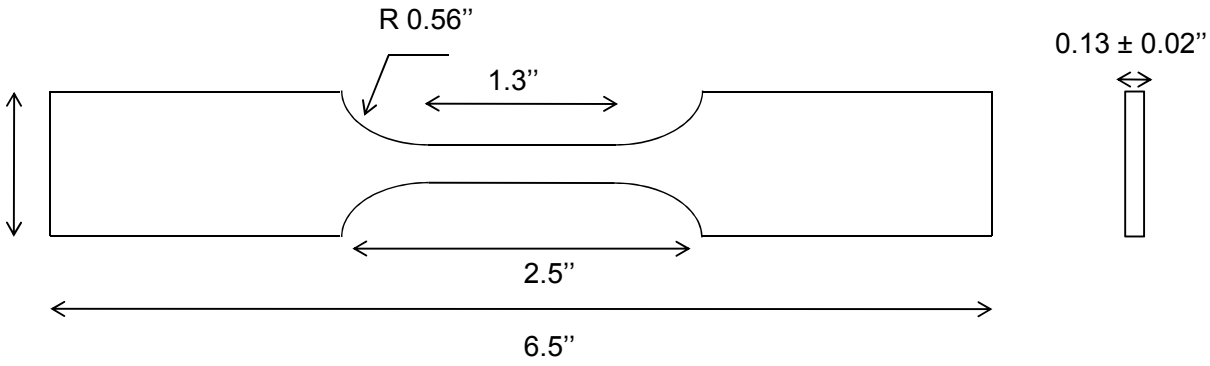

Figure 3-16. Dimensions of the tensile specimen.

4.0 SUMMARY

The Xilinx V4 is a strong candidate for the next-generation FPGA for NASA applications. The major concern regarding the V4 is its non-hermeticity. Due to the non-hermeticity, the underfill material, LP2, will be directly exposed to the LEO environment, albeit within a spacecraft, during the mission. A variety of reliability testing has been performed on the V4; however, there are no test results directly relating reliability and performance to the LEO environment. The goal of the present task was to study reliability of the V4 package in terms of the underfill material under the LEO environment. During FY11, raw LP2 underfill material was procured and went through a series of tests to measure its properties and to study its behavior. We have confirmed that properties such as Tg, CTE, Young's modulus, and lap shear strength of the LP2 underfill are suitable for high-reliability ceramic flip chip package applications. We also confirmed that the LP2 underfill material maintains high lap shear strength under a wide range of temperatures relevant to space applications. The LP2 underfill material has good outgassing reliability under both vacuum thermal cycling and radiation environment. We have not found any significant weakness in the LP2 material. Since most of the tests were done under atmospheric pressure, we will continue to perform additional tests in FY12 to verify the long-term reliability of the LP2 underfill in the LEO environment.

5.0 REFERENCES

[1] Ramin Roosta, "Qualification & Screening Issues of Xilinx Virtex-4 FPGAs for Space Applications," A presentation at Microelectronics Reliability & Qualification Workshop (MRQW), Dec. 2009.

[2] K. N. Tu, "Solder Joint Technology: Materials, Properties, and Reliability," Springer, 2007.

[3] J. Clech, J. C. Manock, D. M. Noctor, F. E. Bader, and J. A. Augis "A Comprehensive Surface Mount Reliability Model Covering Several Generations of Packaging and Assembly Technology" , IEEE Transactions on Components, Hybrids, and Manufacturing Technology, vol. 16, no. 8, pp. 949, 1993.

[4] J. W. Nah, J. O. Suh, K. N. Tu, S. W. Yoon, V. S. Rao, V. Kripesh, and F. Hua, "Electromigration in flip chip solder joints having a thick Cu column bump and a shallow solder interconnect," Journal of Applied Physics, vol. 100, no. 12, 123513, 2006.

[5] W. Engelmaier, "Generic Reliability Figures of Merit Design Tools for Surface Mount Solder Attachments," IEEE Transactions on Components, Hybrids, and Manufacturing Technology, vol. 16, no. 1, pp. 103, 1993.

[6] S.L. Buchwalter, M.E. Edwards, D. Gamota, M.A. Gaynes, and S.K. Tran, "Underfill: The Enabling Technology for Flip-Chip Packaging," in Area Array Interconnection Handbook, eds. K. J. Puttlitz, and P. A. Totta, Springer, 2001.

[7] J. Clementi, J. McCreary, T.M. Niu, J. Palomaki, J. Varcoe and G. Hill, "Flip chip encapsulation of ceramic substrates," in Proc. 43rd Electronic Comp., Technol. Conf., pp. 175, 1993.

[8] D. L. Edwards, B.C. Campbell, J.H. Covell Jr., K.C. Marston, C. Proietti-Bowne," Manufacturing Considerations and Tools for Flip Chip, Assembly," in Area Array Interconnection Handbook, eds. K. J. Puttlitz, and P. A. Totta, Springer, 2001.

[9] V. Gektin, A. Bar-Cohen, and J. Ames, "Coffin-Manson Fatigue Model of Underfilled Flip-Chips," IEEE Transactions on Components, Packaging, and Manufacturing Technology—part A, vol. 20, no. 3, September 1997.

[10] C.A. Handwerker, F. W. Gayle, E. E. de Kluizenaar, and K. Suganuma, "Major International Lead (Pb)-Free Solder Studies" in Handbook of lead-free solder technology for microelectronic assemblies, eds. K. J. Puttlitz and K. A. Stalter, 2004.

[11] T. Siewert, S. Liu, D.R. Smith, and J.C. Madeni, NIST Database for Solder Properties with Emphasis on New Lead-free Solders Release 4.0, 2002.

[12] E. Grossman and I. Gouzman, "Space environment effects on polymers in low Earth orbit," Nuclear Instruments and Methods in Physics Research B, vol. 208, pp. 48, 2003.

[13] H. W. Bonin, V. T. Bui, H. Pak, E. Poirier, H. Harris, "Radiation Effects on Aluminum-Epoxy Adhesive Joints," Journal of Applied Polymer Science, vol. 67, pp. 37, 1998.

[14] T. W. Wilson, R. E. Fornes, R. D. Gilbert, and J. D. Memory, "Effect of Ionizing Radiation on the Dynamic Mechanical Properties of an Epoxy and a Graphite Fiber/Epoxy Composite," Journal of Polymer Science pt. B, Polymer Physics, vol. 26, pp. 2029, 1988.

[15] I.J. Rasiah, "Selecting an underfill for flip chip packaing," Electronics Engineer, 1999.

[16] K. Darbha, J.W.Okura and A.Dasgupta, "Impact of Underfill Filler Particles on Reliability of Flip Chip Interconnects," IEEE Transactions on Components, Packaging, and Manufacturing Technology pt. A, vol. 21, no. 2, pp. 275, 1998.

[17] P. Su, S. Rzepka, M Korhonen, and C.Y. Li , "The Effects of Underfill on the Reliability of Flip Chip Solder Joints," Journal of Electronic Materials, vol. 28, no. 9, pp. 1017, 1999.

[18] K. Nagarajan and R. H. Dauskardt, "Adhesion and reliability of underfill/substrate interfaces in flipchip BGA packages: Metrology and characterization," in Proc. SEMICON West Electron. Manuf. Technol. Symp., pp. 206, 2002.

[19] L.C. Wang and R.H. Dauskardt, "Effect of Composition and Bead Settling on Debonding of Underfill Layers," Microelectronics and Microsystems Packaging Mat. Res. Soc. Symp. Proc., vol. 682E. N1.7. 1-6, 2002.

[20] S.K. Kang, Peter Gruber, and Da-Yuan Shih, "An overview of Pb-free, flip-Chip Wafer-Bumping technologies," Journal of The Minerals, Metals And Materials Society, vol. 60, no. 6, pp. 66-70, 2008

[21] M.H. Tsai, W.M. Chen, M.Y. Tsai, C.R. Kao, "Sn concentration effect on the formation of intermetallic compounds in high-Pb/Ni reactions," Journal of Alloys and Compounds, vol. 504, pp.341, 2010.

[22] B. Han and Y. Guo, “Thermal deformation analysis of various electronic packaging products by Moiré and microscopic Moiré interferometry,” Journal of Electronic Packaging, vol. 117, No. 3, pp. 185-191, 1995.

[23] A. T. Wu, C. Y. Tsai, C. L. Kao, M. K. Shih, Y. S. Lai, H. Y. Lee, C. S. Ku, “In Situ Measurements of Thermal and Electrical Effects of Strain in Flip-Chip Silicon Dies Using Synchrotron Radiation X-rays,” Journal Of Electronic Materials, vol. 38, no.11, pp. 2308-2313, 2009.

[24] J. H. Lau, “Solder joint reliability of flip chip and plastic ball grid array assemblies under thermal, mechanical, and vibrational conditions,” IEEE Transactions on Components, Packaging, and Manufacturing Technology part B, vol. 19, no. 4, pp. 728-735, 1996.

[25] W. C. Oliver and G. M. Pharr, “An improved technique for determining hardness and elastic modulus using load and displacement sensing indentation experiments,” Journal of Materials Research, vol. 7, pp. 1564-1583, 1992.

[26] L. Fan, C. Tison, and C. P. Wong, “Adhesion of Underfills toward TinLead and Lead-Free Solders,” Proceeding in IEEE 8th International Symposium on Advanced Packaging Materials, pp. 291, 2002.

[27] Draft 7 of IPC standard J-STD-030, “Guideline for Selection and Application of Underfill Material for Flip Chip and other Micropackages.”

[28] M. S. Anderson, et al., “Analysis of Semi-Volatile Residues Using Diffuse Reflectance Infrared Fourier Transform Spectroscopy,” in Optical System Contamination: Effects, Measurements, and Control VII; July 2002, edited by Phillip T. C. Chen and O. Manuel Lee; Proceedings of the SPIE, vol. 4774, pp. 251-261, 2002.

[29] D. M. Taylor, D. M. Soules, and D. Osborn , “JPL Molecular Contamination Investigation Facility,” Proceedings of SPIE, vol. 1329, pp. 233-244, 1990.

[30] C. E. Park, B. J. Han, and H. E. Bair, “Humidity effects on adhesion strength between solder ball and epoxy underfills,” Polymer, vol. 38, no. 15, pp. 3811-3818, 1997.